Behavior of Repaired Cyclically Loaded Shearwalls

by Frank J. Vecchio, Omar A. Haro de la Peña, Filippo Bucci, and Daniel Palermo

Two large-scale, wide-flanged shear walls were subjected to reversed cyclic displacements, resulting in the web elements sustaining heavy damage. The walls were repaired by removing and replacing the damaged concrete, and then were reloaded. Test results indicate that there can be a near full restoration of the walls' strength, stiffness, and energy dissipation characteristics. However, it is shown that the repair scheme, strength of the repair concrete, and residual damage in the unrepaired zones can have a significant influence on subsequent behavior, particularly in altering the mode of failure. It is also shown that properly accounting for previous loading, residual damage, and repair sequence is critical to obtaining accurate predicted responses from analytical procedures. The data from this test series, augmenting other data available in the literature, will be useful in calibrating improved analytical methods as they are developed.

Keywords: concrete; repair; shearwalls; test.

INTRODUCTION

Expenditures related to the repair and rehabilitation of reinforced concrete infrastructure in North America now rival those of new construction. This may be due to a number of reasons including the age of our infrastructure, structures designed to meet past standards that are now deemed inadequate or unsafe, exposure to aggressive environments or extreme loads, or changes in function requirements. Consequently, much research effort has been directed in recent years to the development and testing of new repair materials and associated technologies. A recent focus among researchers is to corroborate the performance of repaired or enhanced structural systems, particularly in the context of satisfying or updating code specifications. The current amount of work relating to fiber-reinforced polymers (FRP) as a repair material is a prime example.

Lagging behind has been complementary work in developing analytical techniques that enable accurate assessments of the performance and safety of repaired structures, or rational assessments of different repair options. From an analytical perspective, a rigorous quantitative assessment of a repaired or rehabilitated concrete structure presents a formidable challenge. Extensive reformulation of nonlinear algorithms is required if one is to rigorously consider changing structural configurations, superposition of previously loaded or damaged portions of a structure with newly added unstressed elements, constitutive behavior of repair materials, and inclusion of residual stresses and strain differentials across repair interfaces. Further, a proper account of the chronology of the loading, damage, and repair sequences is often critical to accurately estimate the anticipated response. Vecchio and Bucci[1] described a nonlinear finite element analytical approach suitable to such applications. Ziraba[2] also reported some success in this regard. Otherwise, little directly relevant research can be found in the literature.

Essential to the development of reliable analytical tools is the availability of test data suitable for corroboration of the theoretical formulations. These data exist for some types of structural components, that is, beams, columns and piers, and beam-column joints.[3-8] In many cases, the experimental investigations described involve elements repaired with externally bonded FRP fabric or plates, steel jackets, or epoxy injection techniques. With respect to shearwalls, Fiorato, Oesterle, and Corley[9] presented a seminal work in which several rectangular and barbell-shaped walls were damaged under cyclic loading, repaired by replacing the damaged concrete, and then retested. In addition, Lefas and Kotsovos[10] provided data on three rectangular walls similarly damaged, repaired, and reloaded. In both investigations, the walls were relatively slender, with height-to-width ratios of 2.0 or greater, and were heavily influenced by flexural mechanisms.

The current body of data would benefit from complementary studies involving squat shearwalls more heavily influenced by shear-related mechanisms. Tests involving more complex wall configurations, in which three-dimensional effects may be influential, are also lacking. If these data were available, the development and verification of theoretical models and procedures suitable for the analysis of repaired structures could proceed with greater confidence.

RESEARCH SIGNIFICANCE

With the increasing emphasis being placed on the development and application of repair materials and techniques, there is an increasing need for complementary analytical tools. The development of these tools, in turn, creates a need for test data by which the immanent material models and analytical procedures can be verified. This paper describes a test program in which large-scale, three-dimensional wall systems were severely damaged under reversed cyclic loading conditions, and were then repaired and reloaded. The main objective is to present data that will be useful in calibration studies. The paper will also show that a proper repair can largely restore the strength, stiffness, and energy dissipation characteristics of a severely damaged wall. Finally, it will be shown that a proper account of previous loading and damage is essential if one is aiming to accurately model the response of a repaired wall.

SPECIMEN DETAILS

The test program undertaken involved four large-scale, wide-flanged squat shearwalls patterned after the type recently tested by the Nuclear Power Engineering Corporation of Japan (NUPEC).[11] (The NUPEC walls were nominally of the same dimensions and reinforcement details, but tested under dynamic load conditions.) Specimens DP1 and DP2, two originally

ACI member **Frank J. Vecchio** *is Professor and Associate Chair in the Department of Civil Engineering, University of Toronto, Toronto, Ontario, Canada. He is a member of Joint ACI-ASCE Committee 441, Reinforced Concrete Columns, and 447, Finite Element Analysis of Reinforced Concrete Structures. His research interests include nonlinear analysis and design of concrete structures, constitutive modeling, assessment, and repair and rehabilitation of structures.*

Omar A. Haro de la Peña *is a professor at the Universidad Panamericana Guadalajara, Mexico, and Chief Structural Engineer at the firm Bufete for Studies and Technical Solutions (BEST), Guadalajara, Mexico. He received his BASc from the Universidad Panamericana and his MASc in structural engineering from the University of Toronto.*

Filippo Bucci *is a design engineer in Milan, Italy. He received his MASc in structural engineering from the University of Toronto.*

Daniel Palermo, *PEng, is a doctoral candidate in the Department of Civil Engineering, University of Toronto. He received his BASc and his MASc from the University of Toronto in 1995 and 1998, respectively. His research interests include constitutive modeling of concrete subjected to cyclic loading and experimental testing of shear walls.*
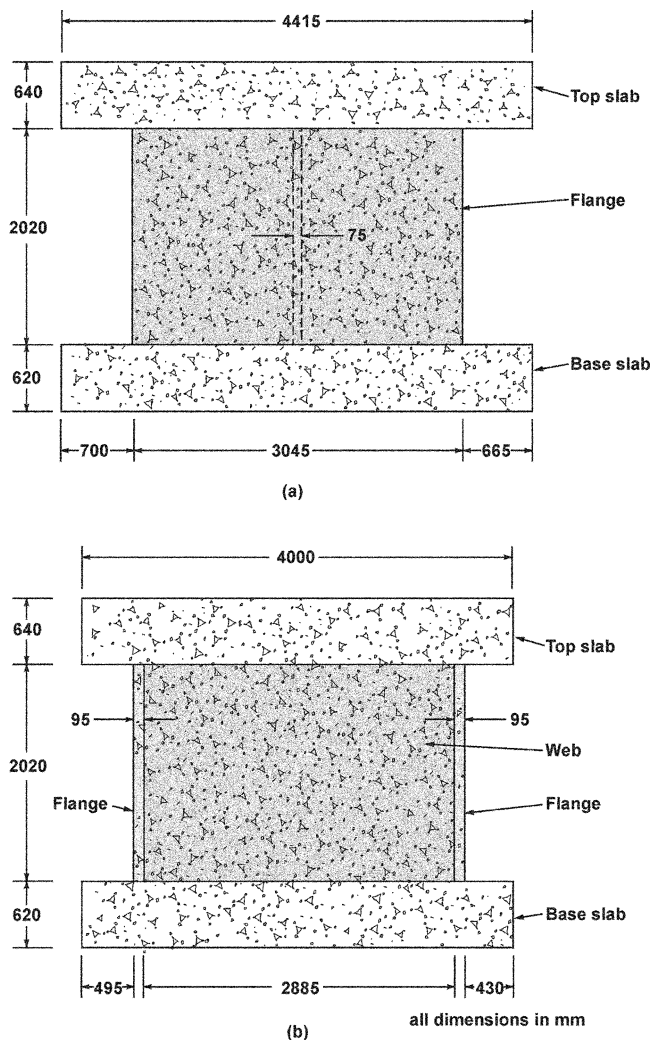
Table 1(a)—Material properties: concrete

Zone	DP1R			DP2R		
	f_c', MPa	ε_o, $\times 10^{-3}$	E_c, MPa	f_c', MPa	ε_o, $\times 10^{-3}$	E_c, MPa
Web (replaced)	44.0	2.50	28,900	39.4	2.15	27,700
Web (original)	21.7	2.04	25,900	18.8	2.12	18,600
Flange wall	21.7	2.04	25,900	18.8	2.12	18,600
Top slab	43.9	1.93	43,700	38.0	1.96	37,600
Bottom slab	34.7	1.66	57,500	34.7	1.66	57,500

Table 1(b)—Material properties: reinforcement

Zone	Type	Diameter, mm	ε_{sy}, $\times 10^{-3}$	f_{sy}, MPa	f_{su}, MPa	E_s, MPa
Web wall	D6	7.0	3.18	605	652	190,200
Flange wall	D6	7.0	3.18	605	652	190,200
Top slab	No. 30	29.9	2.51	550	696	219,100
Bottom slab	No. 30	29.9	2.51	550	696	219,100

the walls were of H-section type, built integrally with stiff top and bottom slabs. In the typical specimen, the storey height, from the top of the base slab to the soffit of the top slab, was 2020 mm. The web sections were 75 mm thick by 2885 mm wide, and the flanges were 3045 mm across. The flange thickness was 95 and 100 mm for Specimens DP1/DP1R and Specimens DP2/DP2R, respectively.

The horizontal reinforcement in the web wall consisted of two layers of D6 deformed bars spaced at 140 mm, giving a reinforcement ratio of approximately 0.73%. The vertical reinforcement in the web consisted of two layers of D6 bars spaced at 130 mm, with a corresponding reinforcement ratio of 0.79%. The flanges were also reinforced with two layers of horizontal D6 bars spaced at 140 mm ($\rho_h = 0.58\%$ for Specimens DP1/DP1R; and 0.55% for Specimens DP2/DP2R). The two layers of vertical D6 bars provided in the flanges were spaced at 130 mm near the web wall joint, and at 355 mm near the flange tips. A clear cover of 15 mm was provided in both the web and flanges. The orthogonally reinforced top and bottom slabs each contained two layers of No. 30 bars spaced at 350 mm in each direction. Reinforcement details are summarized in Fig. 2. (Note: The diameter of a D6 bar is 7.0 mm, and that of a No. 30 bar is 29.9 mm.)

It should be noted that the original walls were built in three stages: first the base slab, then the web and flanges, and finally the top slab, with appropriate measures taken to ensure continuity of the reinforcement and good bond between the concrete sections. For the repaired walls, as will be discussed later, the web section concrete was removed and replaced. Note that there is a variation in the strength of the concrete found in the various components of each specimen. The concrete material properties for components of the two repaired walls are given in Table 1(a). The properties of the reinforcing steel are given in Table 1(b).

The testing apparatus used to apply combinations of lateral and axial loads to the wall specimens is illustrated in Fig. 3. The base slab of the test specimen was post-tensioned to the laboratory strong floor. Axial loads were applied by means of four 600 kN actuators, fixed to the strong floor and reacting against two spreader beams lying across the top slab. Lateral displacements were applied to the top slab by two 1000 kN

Fig. 1—Details of shearwall specimens: (a) end view; and (b) side view.

undamaged specimens, were subjected to quasi-static reversed cyclic loading. Displacement amplitudes were progressively increased until load capacity was exhausted and the walls had sustained considerable damage. The walls were then repaired and retested as Specimens DP1R and DP2R, respectively. Palermo and Vecchio[12] provide full details of the original specimens' test conditions and results. This paper is concerned with the details and results of the repaired specimens.

All walls were similar in terms of configuration, overall dimensions, and reinforcement details. As shown in Fig. 1,

servo-controlled actuators reacting against a strong wall. The mid-height of the top slab served as the reference point for monitoring the imposed displacements.

All specimens were instrumented with an array of mechanical strain gage targets to measure concrete surface strains, linear variable displacement transducers (LVDTs) to measure displacements, and electrical resistance strain gages to measure strains in the reinforcement. Load cells on each of the six actuators were used to monitor the applied forces. Lateral loads were typically applied as 1 mm increments in top slab displacement. Each displacement level was held for five minutes to allow cracks to be measured and marked, photographs taken, and mechanical strain gage readings made. Computer data acquisition systems provided continuous monitoring and recording of all strain gage, LVDT, and load cell readings. Palermo,[13] Bucci,[14] and Haro de la Peña[15] provide full details regarding specimen construction, instrumentation, and loading procedure.

PREVIOUS DAMAGE AND REPAIR

Specimen DP1 was subjected to a constant axial load of 1200 kN, and incrementally increasing reversed cyclic lateral displacements. The wall was able to sustain a maximum lateral load of 1298 kN, at a corresponding lateral displacement of 11.1 mm. Loading was continued well into the postpeak range of response, with the lateral load resistance decaying to approximately 580 kN at a displacement of 15 mm. The wall sustained severe and widespread crushing of the concrete in the web, with the final failure mechanism involving the formation of six vertical slip planes within the web. Some local yielding of the horizontal reinforcement in the web was recorded; however, no yielding of any vertical reinforcement in the web was detected. The flange walls experienced some flexural cracking, up to widths of 1.1 mm, but remained relatively undamaged. There was no evidence of any concrete distress nor was yielding of either the horizontal or vertical reinforcement detected. The load-displacement response curve for Specimen DP1 is given in Fig. 4(a). Palermo[13] gives a full discussion of the test results.

Specimen DP1 was repaired by completely removing and replacing the concrete in the web component of the wall, while ensuring that the vertical and horizontal reinforcements were preserved without damage. The damaged web concrete was removed with a small pneumatic chipping hammer to within about 15 mm of the flange and top and bottom slab joint regions. The wall was then reformed and recast to a height of 180 mm from the soffit of the top slab. The top zone of the web was later completed using a high-strength, nonshrink epoxy grout in order to achieve proper bond and continuity. A schematic presentation of the repair zone is given in Fig. 5(a). Bucci[14] provides full details of the repair procedure. The repaired wall was designated as Specimen DP1R.

Specimen DP2 was subjected to the same reversed cyclic lateral displacement regime as Specimen DP1, but with no axial load applied other than the dead weight of the top slab. A maximum lateral load of 904 kN was recorded during the first excursion to 9 mm displacements. The ensuing postpeak behavior was found to be nonductile, with a sudden loss in capacity occurring during the first cycle to 10 mm. The failure mechanism primarily involved a sliding shear failure of the concrete in a horizontal plane just below the top slab. The concrete was extensively damaged elsewhere as well, mostly in the corner toe region of the web. Also
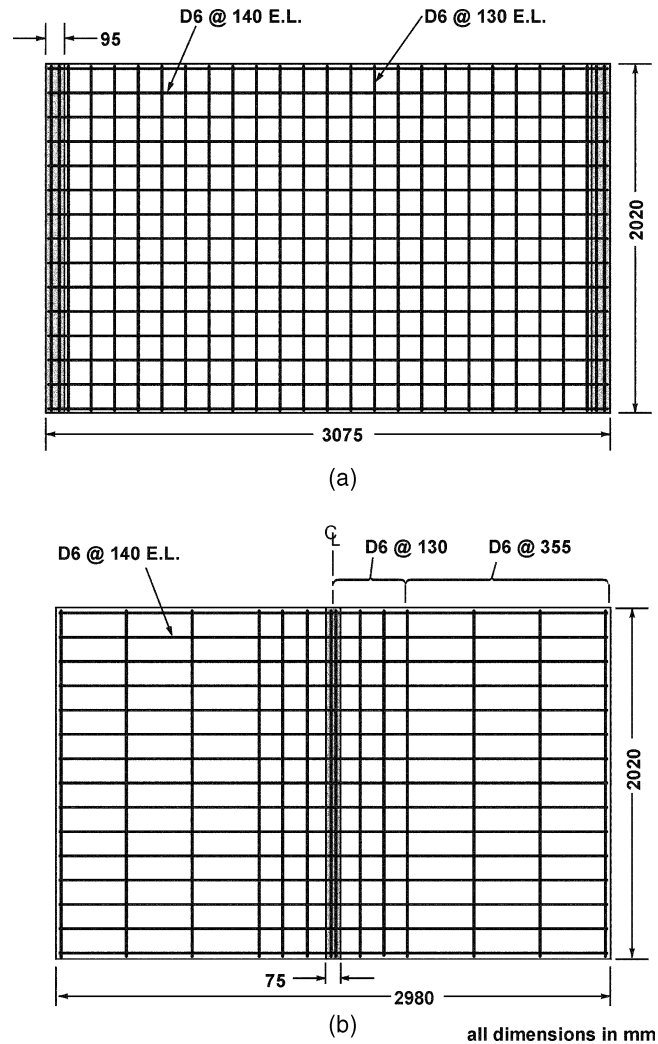

(a)

(b)

all dimensions in mm

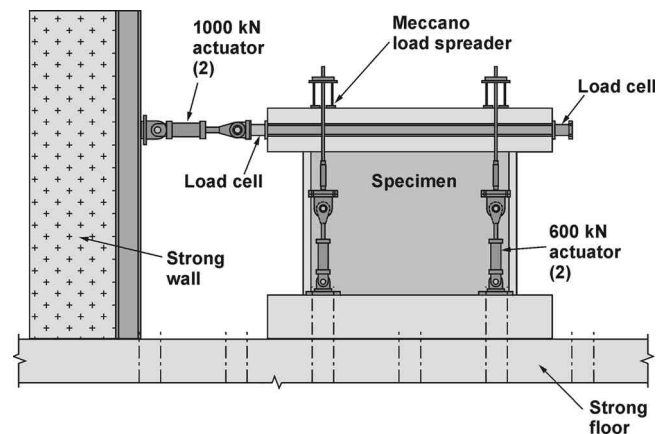Fig. 2—Reinforcement details of (a) web; and (b) flanges.

Fig. 3—Test setup.

significant was the pronounced damage in the web-flange joint regions, with notable punching of the web through the flanges. Yielding of the reinforcement was not detected anywhere in the web or flanges by the electrical strain gages. Concrete surface strain readings, however, indicated probable local yielding of the flange vertical reinforcement. Flexural cracks in the flanges approaching 1 mm width further suggested local yielding had occurred. The load-displacement response curve for Specimen DP2 is given in Fig. 4(b).
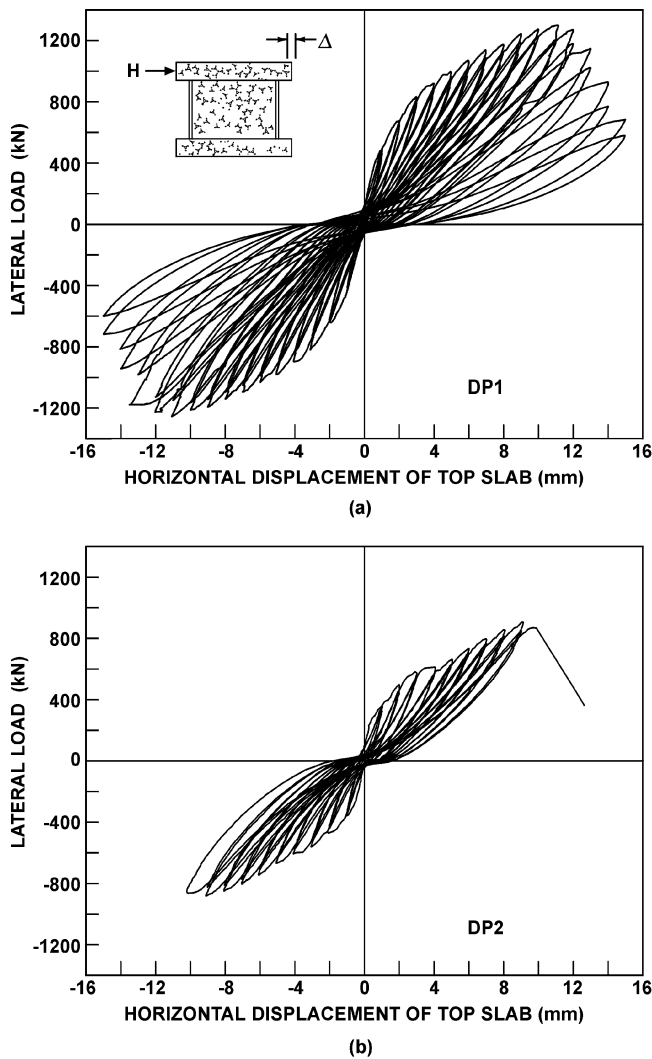
Fig. 4—Load-displacement responses of original walls: (a) Specimen DP1; and (b) Specimen DP2.

Fig. 5—Repair schemes of walls: (a) Specimen DP1R; and (b) Specimen DP2R.

Palermo[13] gives a full discussion of the test results. The repair of Specimen DP2 was performed in much the same manner as Specimen DP1. The web concrete was completely removed, but the web reinforcement was left intact. The major difference, necessitated by the punching failure of the flanges at the web joint, was partial removal of the flange concrete as well. This removal was confined to a width of 750 mm, over the full height of the flanges (Fig. 5(b)). Fresh concrete was placed in the web and web-flange joints, and a high-strength, non-shrink epoxy grout was used for the top 180 mm of the wall. Haro de la Peña [15] provides full details of the repair procedure. The repaired wall was designated as OHSW1. For the purposes of this paper, it will be referred to as Specimen DP2R.

It should be noted that with Specimens DP1R and DP2R, the compressive strength of the replacement concrete in the webs was about double that of the original concrete in Specimens DP1 and DP2, respectively.

TEST CONDITIONS AND RESULTS

Specimens DP1R and DP2R were both preloaded and tested under constant axial loads of 1200 kN (including the weight of the top slab), representing a uniform axial stress on the web and flange walls of approximately 1.5 MPa. Specimen DP1R was subjected to reversed cyclic lateral
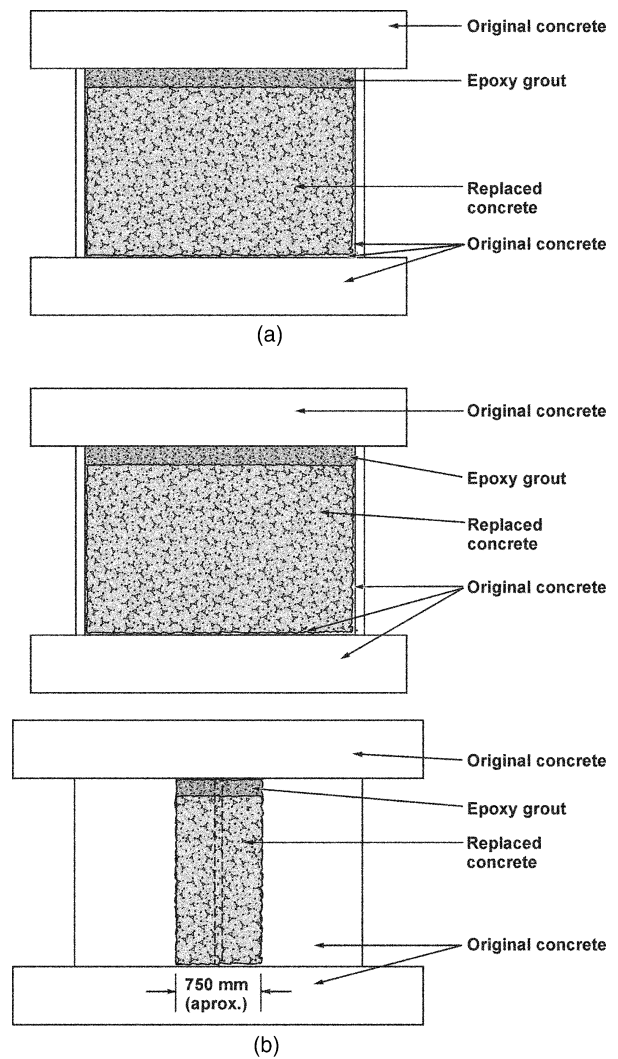
displacements applied to the top slab; the displacement amplitude was progressively increased by 1 mm, with two cycles applied at each amplitude level. (Hence, the loading of Specimen DP1R was identical to that of Specimen DP1.) Specimen DP2R was subjected to monotonically increasing lateral displacement. (The difference in loading conditions for Specimens DP1R and DP2R was chosen to provide a broader base of comparison for corroborating analytical procedures.)

In the testing of Specimen DP1R, web shear cracks became apparent at displacements as low as 1.0 mm, much sooner than evident in the original wall (Specimen DP1). Owing to the precracked nature of the flange walls, lateral load stiffness at low displacement levels was somewhat reduced. Post-cracking stiffness at intermediate load levels, however, was comparable to that of the original wall. (Note that the strength of the web concrete in the repaired wall, however, was 44.0 MPa, as opposed to 21.7 MPa in the original wall.) At a displacement amplitude of 7.0 mm, the web was extensively cracked throughout, with maximum crack widths of 0.5 mm recorded. Crack patterns and crack widths, measured using a surface gage with a precision of 0.05 mm, remained essentially stable thereafter. During the first excursion to 11 mm (0.55% drift), the maximum load capacity of 1192 kN was achieved. Figure 6(a) shows the condition of the wall at this load stage. Load resistance gradually diminished
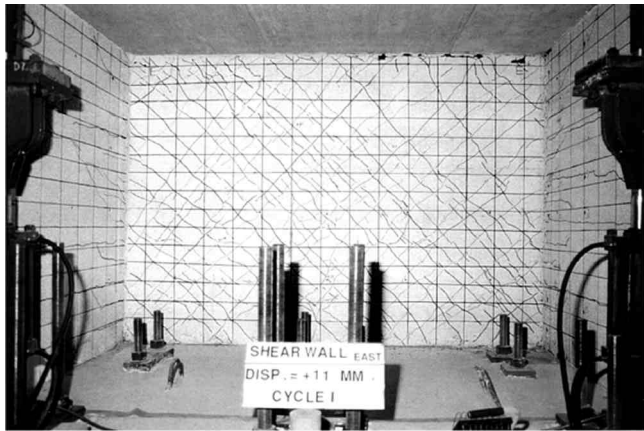
(a)

(b)

Fig. 6—Specimen DP1R: (a) at ultimate load; and (b) at failure.

Fig. 7—Load-displacement responses of repaired walls.

thereafter. At displacement amplitude of 17 mm, the load resistance decayed to approximately 350 kN. The load-deformation response, reproduced in Fig. 7, was characterized by highly pinched hysteresis curves indicative of shear-dominated behavior. Crushing and localized spalling of the concrete was noted at displacement levels of 11 mm and above. At 12 mm displacement, the first signs of a potential punching of the web through the base of the flanges became evident. Finally, at 17 mm displacement (0.85% drift), the wall sustained a sliding shear failure along the base (just above the repair interface), coupled with punching of the web through the flanges (Fig. 6(b)). Minor localized yielding of the vertical reinforcement, in both the web and flanges, was observed in the postpeak response. Bucci[14] provides a full description of the test results.

Specimen DP2R demonstrated considerably greater strength and ductility than did Specimen DP2, which can be explained by the influence of the axial load, the much higher strength of the web concrete (39.4 and 19.4 MPa in Specimens DP2R and DP2, respectively), and the loading conditions (monotonic versus reversed cyclic lateral loads). The load-deflection response curve obtained is shown in Fig. 7. Again, owing to the precracked condition of the flanges, there was some initial softness in the deflection response and a gradually reducing stiffness. The maximum load resistance attained was 1610 kN, occurring at a displacement of 15.8 mm. As seen in Fig. 8(a), the web was extensively cracked by this stage, with shear cracks ranging in width up to 0.5 mm. Thereafter, noticeable decay in the load resistance was observed until a sudden loss
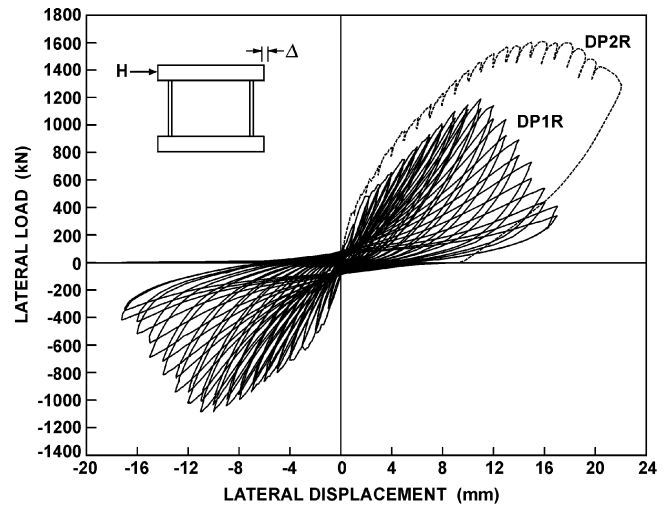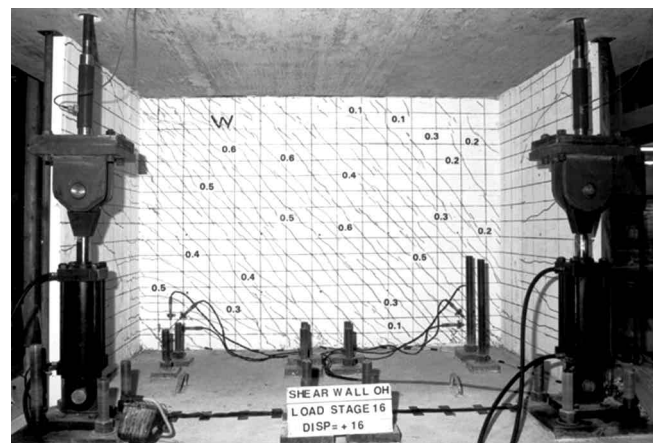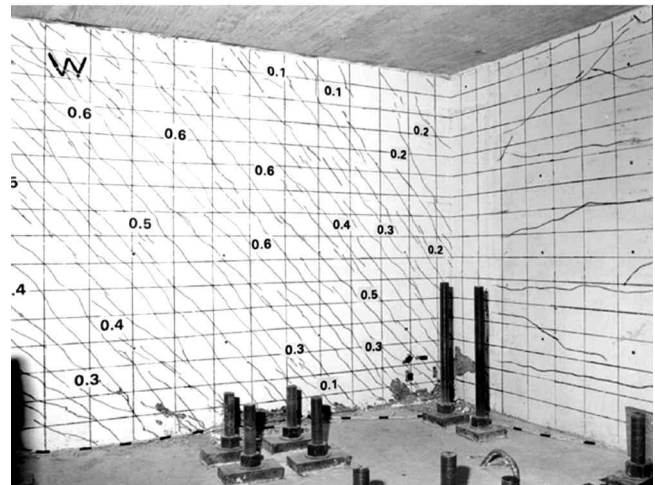

(a)

(b)

Fig. 8—Specimen DP2R: (a) at ultimate load; and (b) at failure.

in capacity occurred at 21 mm displacement. At maximum load, widespread crushing and some spalling of the concrete was observed, particularly in the compression toe region of the web. The final failure mechanism involved compression strut crushing, sliding shear along a horizontal plane above the repair interface, and punching of the web through the compression flange (Fig. 8(b)). There had been evidence of
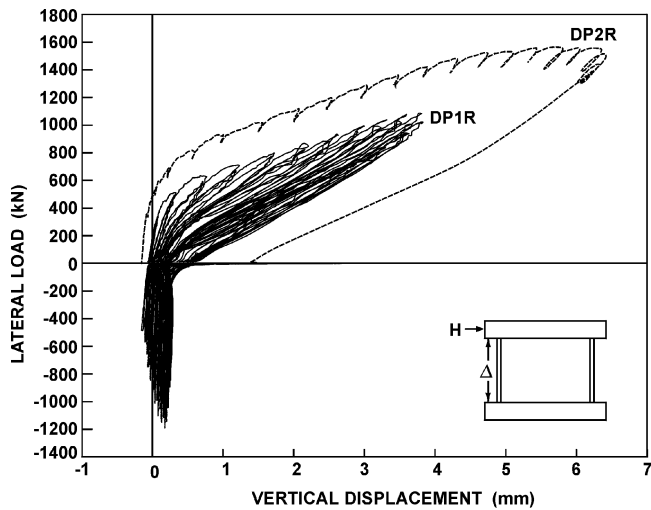
Fig. 9—Flange elongation.

Fig. 10—In-place expansion of web at midheight.

web punching as early as 5 mm displacement, with vertical cracks appearing on the outside surface of the flange directly over the web joint. First yielding of the vertical and horizontal reinforcement in the web was noted at displacement levels of 13.6 and 16.9 mm, respectively. First yielding of the vertical reinforcement in the tension flange occurred at a displacement level of 10.8 mm. Haro de la Peña[15] provides a full description of the test results.

The test data that are especially useful in understanding behavior and corroborating analytical models are those of a second-order nature, describing subtleties in response. Among them is the elongation of the flange walls, particularly in walls subjected to reversed cyclic loading where ratcheting (due to reinforcement yielding) may be prevalent. Figure 9 shows the progressive elongation of one of the flange walls in Specimen DP1R. Elongation of the tension flange in Specimen DP2R is also shown. Note that in the postpeak response of Specimen DP1R, as the resistance force diminishes with increased lateral displacements, there is some accumulation in the residual displacement. The effect is minor, however, and suggests that yielding of the reinforcement, if any, was minimal. The increasing flange elongation in the postpeak response of Specimen DP2R, however, confirms the influence of yielding.

Another important second-order mechanism is that of the in-plane horizontal expansion of the web wall at midheight. As previously discussed by Vecchio,[16] capturing this behavior in nonlinear finite element analyses is critical to accurately calculating the load capacity and failure mode of the structure. Figure 10 shows the web expansions measured in Specimens DP1R and DP2R. (The expansion was determined from the difference in readings from two horizontal extensometers placed on either edge of the web. See sketch in Fig. 10.) Note that even in the postpeak load stages, the wall continued to expand.

The walls were instrumented with LVDTs to measure any bond slip at the base of the tension flanges; that is, arising from pullout of the vertical reinforcing bars from the base slab, measured in the region of the web/flange joint. (Note: In Specimens DP1 and DP1R, the D6 vertical bars in the web and flanges were anchored to a depth of 570 mm into the base slab, and then bent at 90 degrees with an additional 500 mm extension. In Specimens DP2 and DP2R, the vertical bars were anchored by drilling 12 mm diameter holes in the base
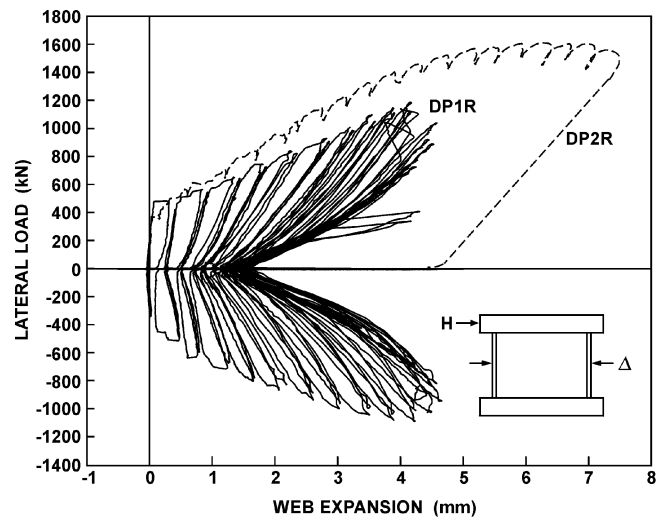
slab, to a depth of 300 mm, and then put in place with epoxy-grouting.) Figure 11 shows the vertical displacement of the flange wall relative to the base, measured at a short height above the base (180 and 200 mm for Specimens DP1R and DP2R, respectively). With both Specimens DP1R and DP2R, comparing Fig. 11 with Fig. 9, one sees that a relatively large proportion of the total flange elongation occurred at the base region. The majority of this displacement appeared as a crack at the base of the wall. Coupling this with the observation that the reinforcement strains were post-yield but not excessive, one may conclude that some amount of bond slip in the anchorage zone of the vertical bars had taken place.

The test walls were also monitored for torsion twisting of the top slab, and for slip of the base slab on the strong floor. In both specimens, there were no significant twists or slips.

DISCUSSION

Although the original walls were subjected to loads well into the postpeak regime and, consequently, severely damaged, effective repair measures were performed. In this study, the repair scheme involved complete removal and replacement of the concrete in the areas of severe damage (that is, the web walls). The repairs did not attempt to remedy any residual detrimental effects from yielding of the reinforcement in either the web or flange elements, extensive cracking of the flanges in tension, or exposure of the concrete in the flanges to high compressive stress values (albeit there was no visible evidence of distress). The repaired walls were able to respond to reloading in a manner approaching that of the previously undamaged walls. Compare the response of Specimens DP1 (Fig. 4(a)) and Specimen DP1R (Fig. 7(a)), recalling that the two walls were subjected to identical loading conditions. One sees almost identical performance in terms of load capacity, pre-peak stiffness, postpeak ductility, and energy dissipation characteristics. A direct comparison between Specimens DP2 and DP2R is more difficult, given the different loading conditions to which the two walls were exposed. The response of Specimen DP2R, however, showed no influence from the previous loading or damage sustained other than a reduced initial stiffness.

At the same time, it should be recognized that the concrete used in the reconstruction of the web walls was approximately twice the strength of the original concrete. This had the effect
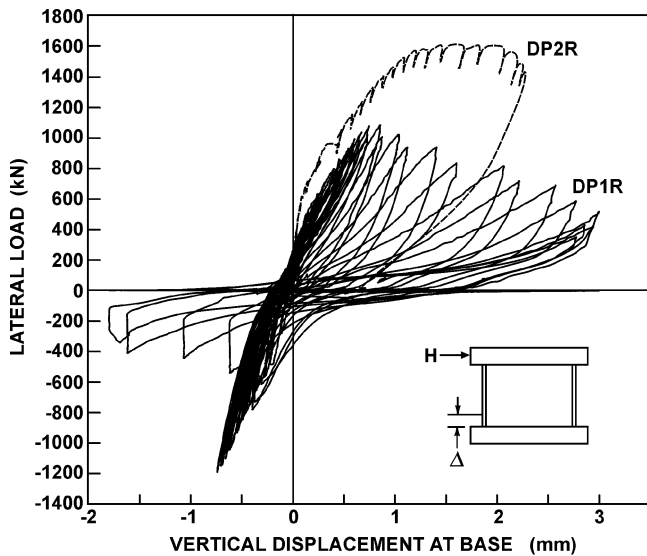
Fig. 11—Vertical displacement at base of flange.

of altering the mode of failure, and possibly the ductility, of the structure. Where punching shear of the web-flange joint was not a principal cause of failure in the original walls, it became a governing factor in the reconstructed walls. Weakness at the repair interfaces, and possible weakness due to residual damage in unrepaired zones, also had some influence on the behavior of the repaired walls. This was most evident in the shear slip plane forming at the base near the repair interface for both walls tested, and in possible weakness in the web-flange joints of Specimen DP1R.

ANALYTICAL MODELING

Vecchio and Bucci[1] previously described a nonlinear finite element procedure aimed at better modelling the behavior of repaired reinforced concrete structures. The proposed method used the concept of plastic strain offsets, coupled with the provision to engage and disengage elements at various stages of loading, in an attempt to properly model the chronology of loading and repair, and the ensuing influence on performance. Preliminary material models describing the nonlinear and load-history dependent behavior of concrete, reinforcement, and various repair materials were incorporated. The procedure was found to be numerically stable and efficient, and adaptable to many practical situations. Applications to cyclically loaded repaired walls showed reasonably good correlations between calculated and observed response,[1] while pointing to some aspects of the modelling that required improvement.

In any attempt to properly model the response of a repaired structure, it is critical to correctly represent the extent of residual stress and damage in elements of the original structure that remain. This becomes evident, for example, when applying the procedure described by Vecchio and Bucci to the analysis of Specimen DP2R. Specimen DP2 (and subsequently Specimen DP2R) was modeled for analysis using a two-dimensional representation of the wall. (Hence, the flange elements were considered acting entirely in-plane with the web, overestimating somewhat both the shear and flexural stiffness of the wall.) Analyses were conducted with loading conditions consistent with those imposed on the test wall; that is, with incrementally increasing lateral displacements up to ±10 mm. At this displacement amplitude, the analytical model indicated less damage than was apparent in the actual wall. The analyses then proceeded with the loading being suspended, the
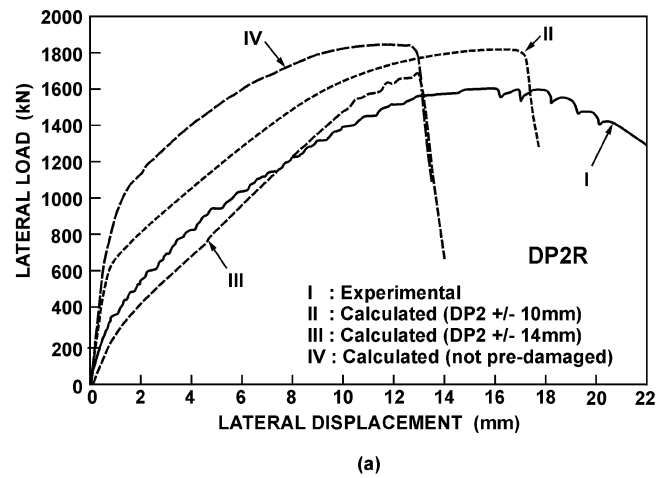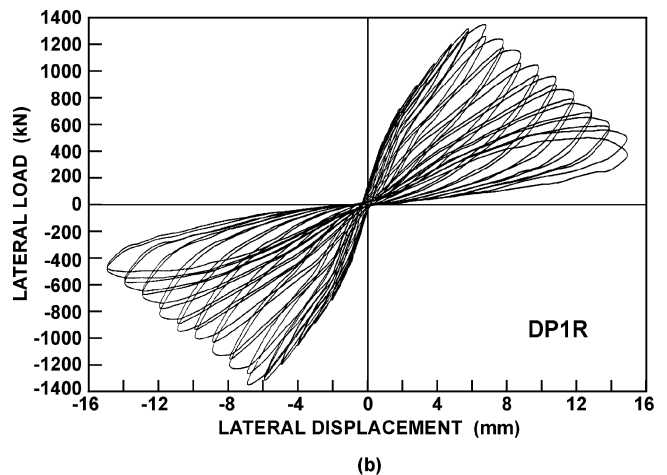
Fig. 12—Calculated load-displacement responses of repaired walls: (a) Specimen DP2R; and (b) Specimen DP1R.

damaged web elements disengaged, new (undamaged) web elements engaged, and the structure reloaded. The experimentally observed response (Curve I) is compared with the resulting calculated load-deflection response (Curve II) in Fig. 12(a). The calculated response is somewhat stiffer and stronger. Some of the discrepancy is attributable to the two-dimensional representation of a structure that, in fact, involves complex three-dimensional behaviors (that is, web-flange punching, shear lag in flanges) but some is also due to the original phase of the analysis underestimating the extent of damage in the structure. The analysis was repeated, pushing the wall to ±14 mm displacement amplitude and hence taking it well into a postpeak (highly damaged) condition. The repair was then simulated and the wall reloaded. The calculated response is shown as Curve III in Fig. 12(a). It is seen that strength and stiffness are more accurately calculated, but the ductility is now underestimated. Hence, overestimating the damage in the original wall resulted in an overly weakened predicted response for the repaired wall, primarily from excessive damage in the flanges. The predicted response, where Specimen DP2R is analyzed as if not previously loaded, damaged, or repaired (that is, new), is shown as Curve IV in Fig. 12(a). A significant overestimation of the strength and stiffness of the wall results, coupled with a more brittle predicted failure mode.

Figure 12(b) shows the cyclic displacement response of repaired Specimen DP1R, computed using a two-stage, two-dimensional finite element analysis (as previously described

for Specimen DP2R). Comparing the calculated response with the experimentally observed response (Fig. 7(a)), the behavior is reasonably well simulated. The final failure mode was also correctly predicted, involving the formation of a sliding shear plane at the base. The slightly overestimated strength and stiffness can be attributed to two factors: the two-dimensional representation of the wall overestimated the contribution of the flanges, and the analysis program used preliminary cyclic loading/unloading and damage models that are in need of further development. Work is progressing in this regard.

CONCLUSIONS

Two large-scale, wide-flanged, shear-critical structural walls were subjected to reversed cyclic lateral displacements into postpeak load regimes. As a result, the web components of the walls sustained severe damage. The walls were repaired by removing and replacing the web concrete, and were then reloaded to failure. Test observations, test data, and analytical studies undertaken in conjunction with the tests, indicated that:

1. Heavily damaged shearwalls can be effectively repaired by removing and replacing of the damaged concrete, with nearly full restoration of strength, postcracking stiffness, ductility, and energy dissipation capacity;

2. Previous loading history, repair sequence, properties of repair materials, and residual damage in unrepaired zones may, nevertheless, affect the subsequent behavior of a wall. In particular, initial stiffness and final failure mode can be significantly altered; and

3. Proper consideration of previous loading and residual damage is essential if analytical procedures are to accurately represent the response of repaired walls.

The data obtained from the tests will be useful in corroborating refined analytical tools as they are developed.

NOTATION

E_c = initial tangent modulus of elasticity of concrete at time of testing
E_s = modulus of elasticity of reinforcement
f_c' = concrete compressive strength at time of testing
f_{sy} = yield stress of reinforcement
f_{su} = ultimate stress of reinforcement
ε_o = concrete strain at peak compressive stress
ε_{sy} = steel strain at yield stress

REFERENCES

1. Vecchio, F. J., and Bucci, F., "Analysis of Repaired Concrete Structures," *Journal of Structural Engineering*, ASCE, V. 125, No. 6, 1999, pp. 644-652.

2. Ziraba, Y. N., "Nonlinear Finite Element Analysis of Reinforced Concrete Beams Repaired by Plate Bonding," PhD thesis, King Fahd University of Petroleum and Minerals, Saudi Arabia, 1993, 326 pp.

3. De Rose, D., "The Rehabilitation of a Concrete Structure using Fibre Reinforced Plastics," MASc thesis, University of Toronto, Toronto, Ontario, Canada, 1997, 177 pp.

4. El-Refaie, S. A.; Ashour, A. F.; and Garrity, S. W., "Strengthening of Reinforced Concrete Continuous Beams with CFRP Composites," *Proceedings of the International Conference on Structural Engineering, Mechanics and Computation*, Elsevier Science, A. Zingoni, ed., 2001, pp. 1591-1598.

5. Haroun, M.; Pardoen, G.; Bhatia, H.; Shahi, H.; and Kazanjy, R., "Structural Behavior of Repaired Pier Walls," *ACI Structural Journal*, V. 97, No. 2, Mar.-Apr. 2000, pp. 259-267.

6. Xiao, Y.; Priestley, M. J.; and Seible, F., "Steel Jacket Retrofit for Enhancing Shear Strength of Short Rectangular Reinforced Concrete Columns," *Report* to the California Department of Transportation, University of California, San Diego, 1993, 192 pp.

7. Bett, B. J.; Klingner, R. E.; and Jirsa, J. O., "Lateral Load Response of Strengthened and Repaired Reinforced Concrete Columns," *ACI Structural Journal*, V. 85, No. 5, Sept.-Oct. 1988, pp. 499-508.

8. French, C. W.; Thorp, G. A.; and Tsai, W., "Epoxy Repair Techniques for Moderate Earthquake Damage," *ACI Structural Journal*, V. 87, No. 4, Jul.-Aug. 1990, pp. 416-424.

9. Fiorato, A. E.; Oesterle, R. G.; and Corley, W. G., "Behavior of Earthquake Resistant Structural Walls Before and After Repair," *ACI Structural Journal*, V. 80, No. 5, Sept.-Oct. 1983, pp. 403-413.

10. Lefas, I. D., and Kotsovos, M. D., "Strength and Deformation Characteristics of Reinforced Concrete Walls under Load Reversals," *ACI Structural Journal*, V. 87, No. 6, Nov.-Dec. 1990, pp. 716-726.

11. Nuclear Power Engineering Corporation of Japan (NUPEC), "Comparison Report, Seismic Shear Wall ISP, NUPEC's Seismic Ultimate Dynamic Response Test," *Report* No. NU-SSWISP-D014, Organization for Economic Co-Operation and Development, Paris, 1996, 407 pp.

12. Palermo, D., and Vecchio, F. J., "Behavior of Three-Dimensional Reinforced Concrete Shear Walls," *ACI Structural Journal*, V. 99, No. 1, Jan.-Feb. 2002, pp. 81-89.

13. Palermo, D., "Behaviour and Analysis of Reinforced Concrete Walls Subjected to Reversed Cyclic Loading," PhD thesis, University of Toronto, 2001.

14. Bucci, F., "Finite Element Analysis of Repaired Concrete Structures," MASc thesis, University of Toronto, 1998, 158 pp.

15. Haro de la Peña, O. A., "Modelling and Analysis of Retrofitted Reinforced Concrete Structures," MASc thesis, University of Toronto, 2001, 242 pp.

16. Vecchio, F. J., "Lessons From the Analysis of a 3-D Concrete Shear Wall," *Structural Engineering and Mechanics*, V. 6, No. 4, 1998, pp. 439-455.